

Figure 11. West-east cross section (a) illustrating relationship between ground surface, aquifer base, and the changing water table in the Ogallala aquifer, and (b) illustration of conceptual model of the aquifer with water input from recharge and water outflow through wells, seepage springs along the escarpment and to rivers.

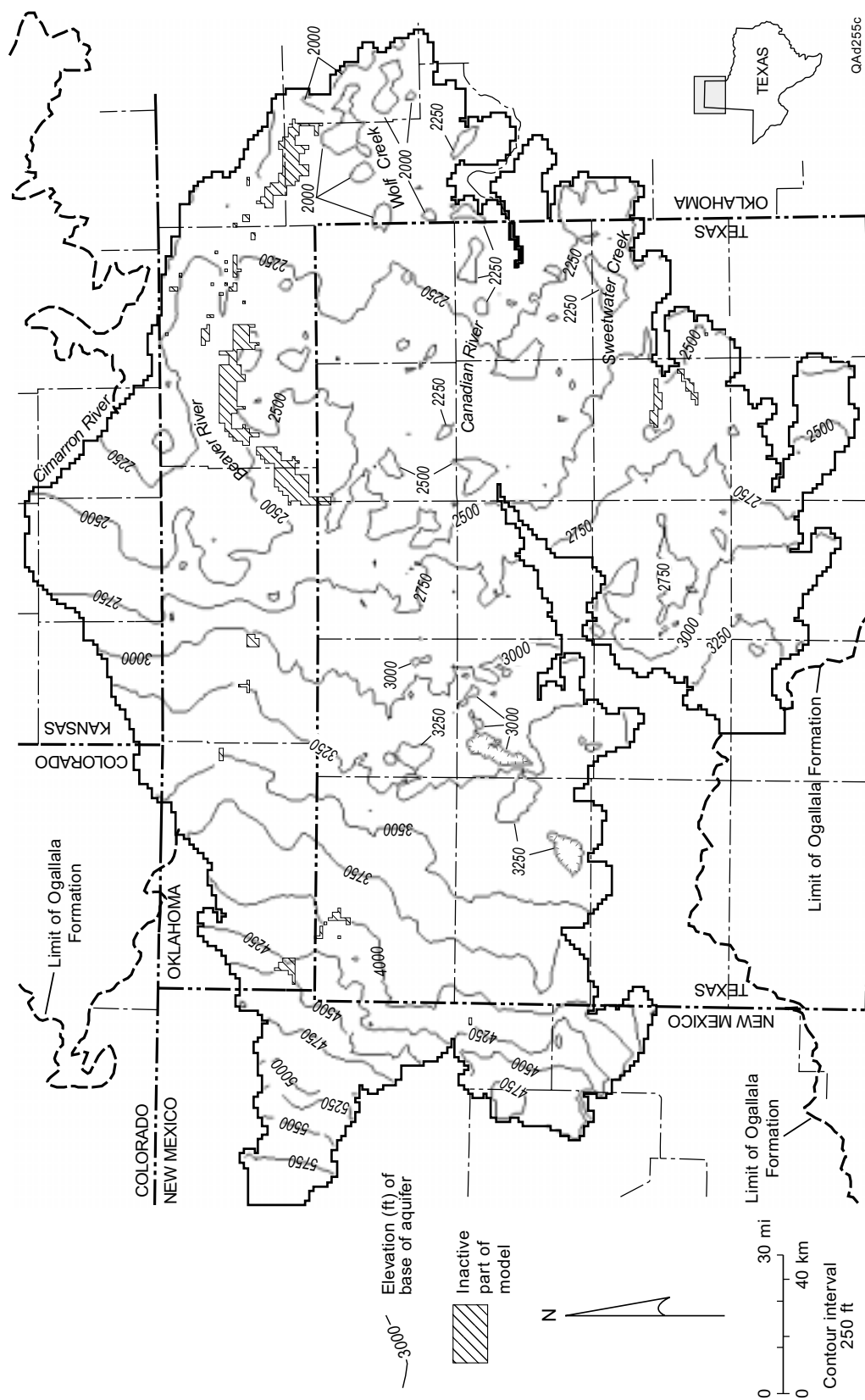


Figure 12. Structural elevation of the base of the Ogallala Formation as used in the numerical model.

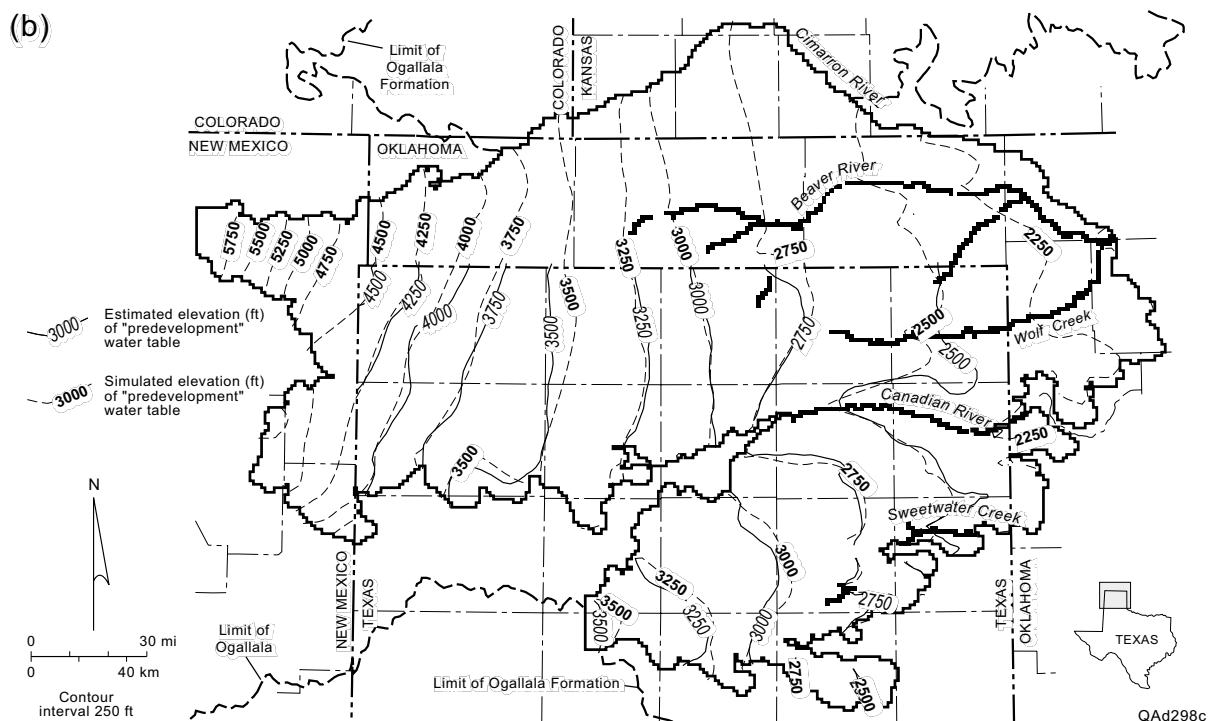
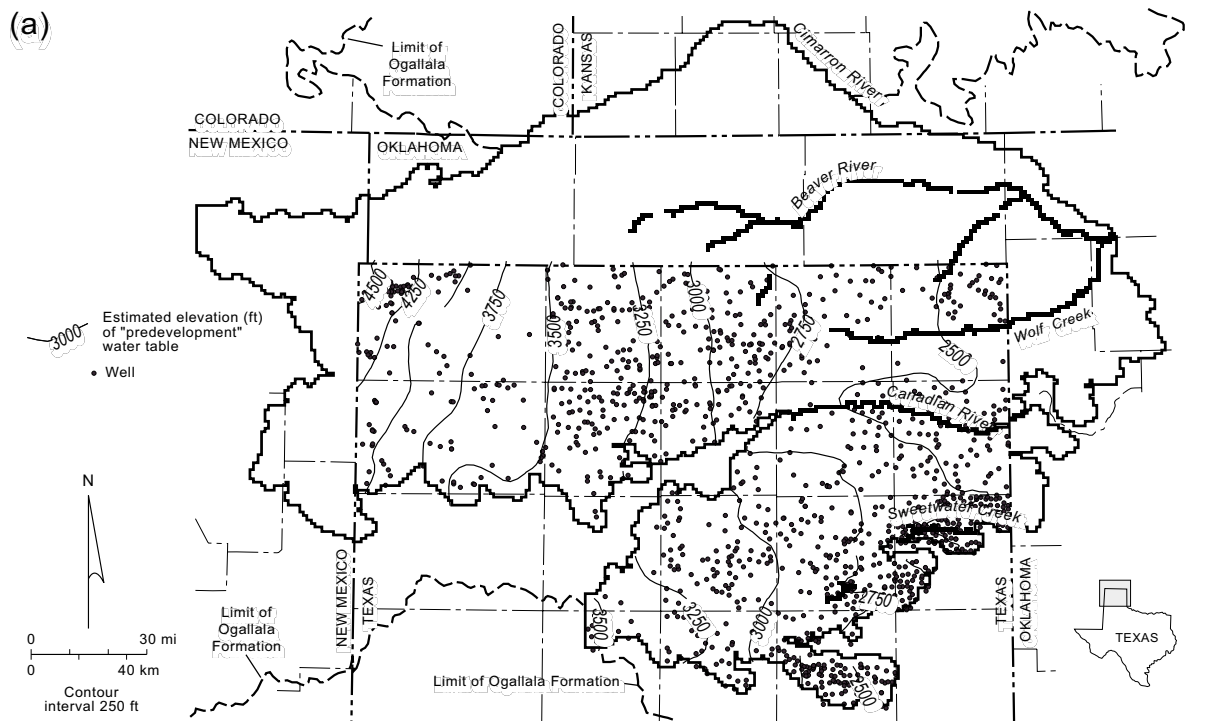


Figure 13. Estimated elevation of "predevelopment" water table (a) and comparison with simulated elevation (b).

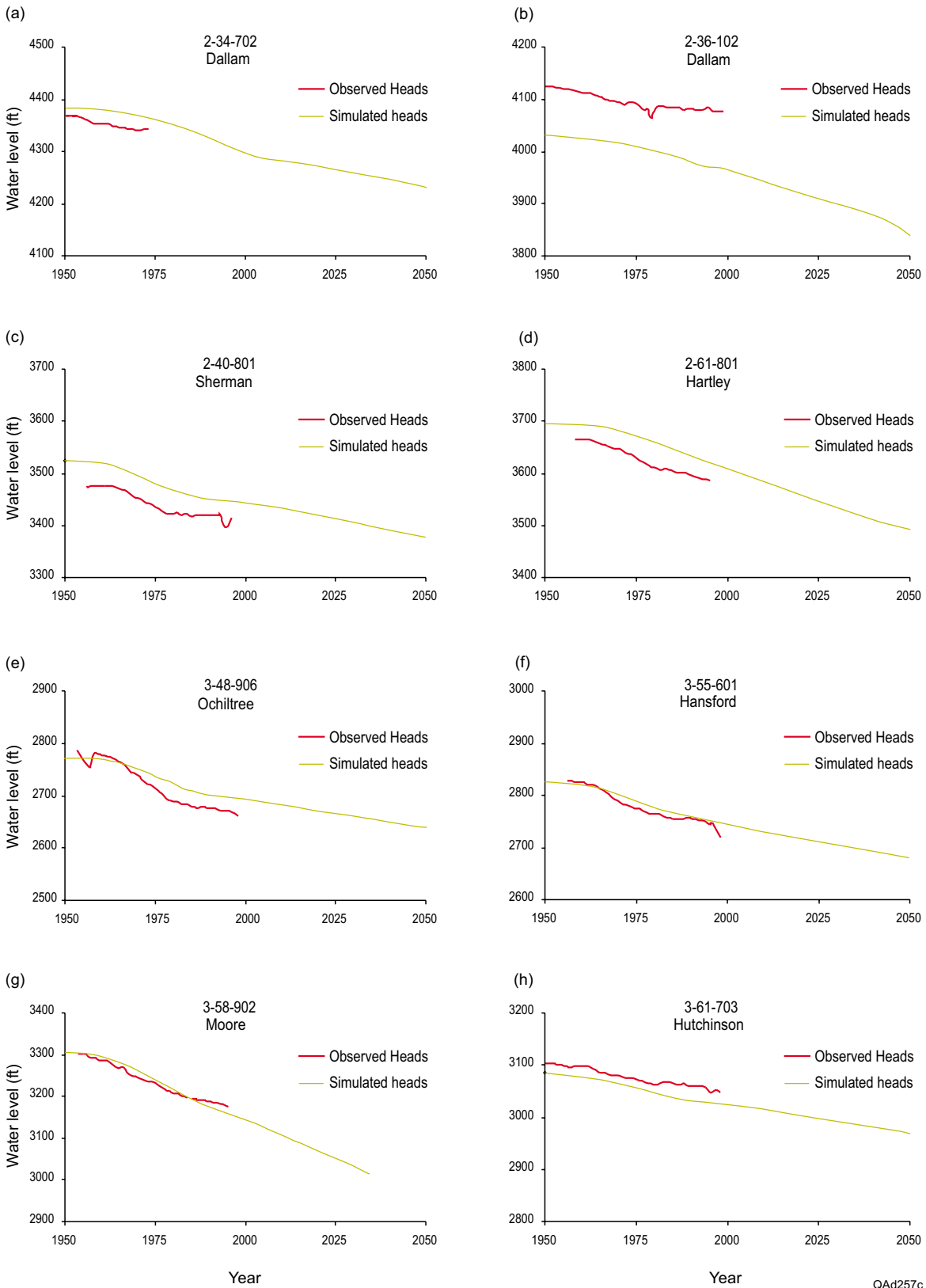
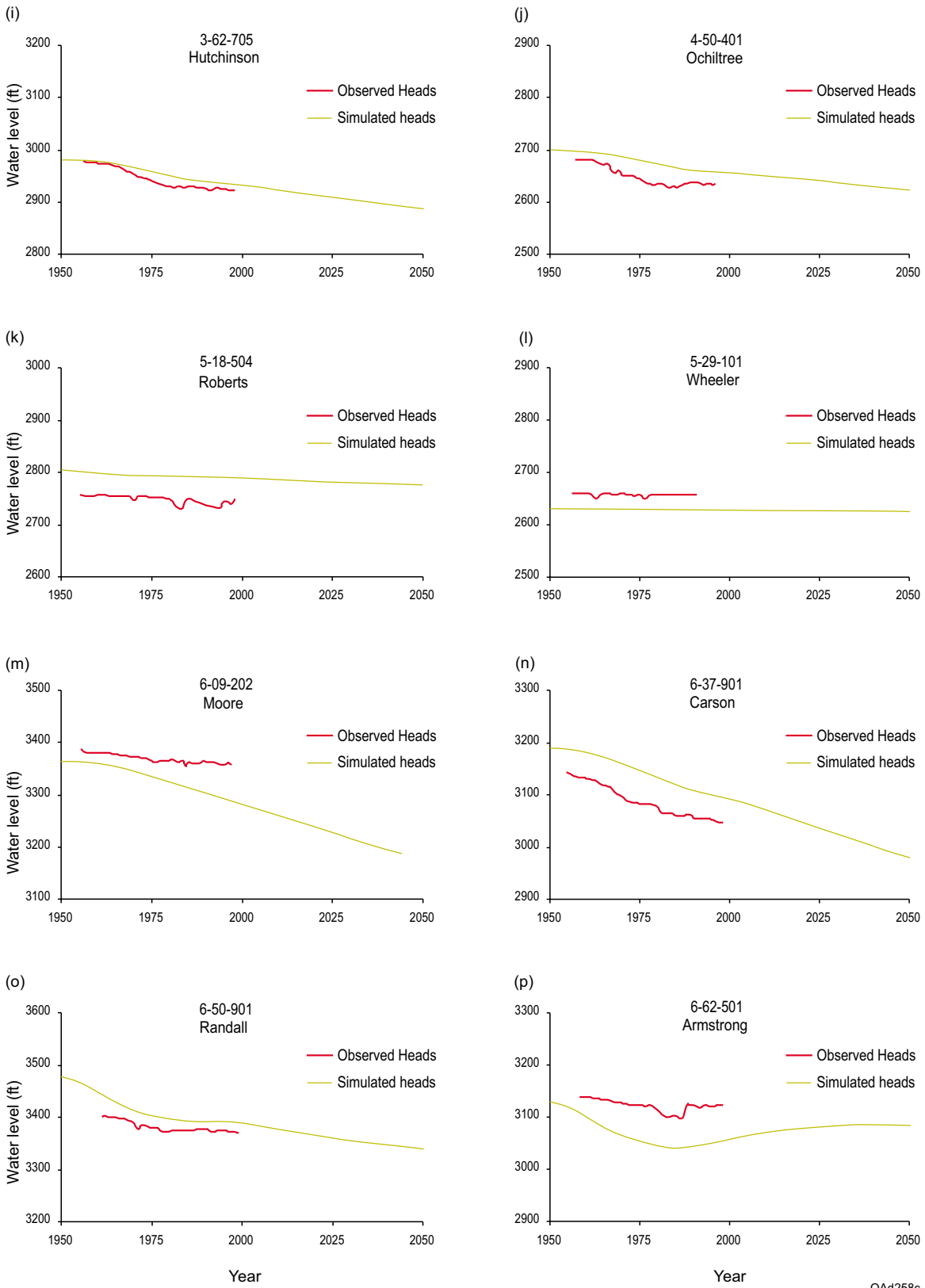


Figure 14. Historical hydrographs demonstrating water-level fluctuations in the Ogallala aquifer. Locations of wells shown in figure 15.



QAd258c

Figure 14 (continued). Historical hydrographs demonstrating water-level fluctuations in the Ogallala aquifer. Locations of wells shown in figure 15.

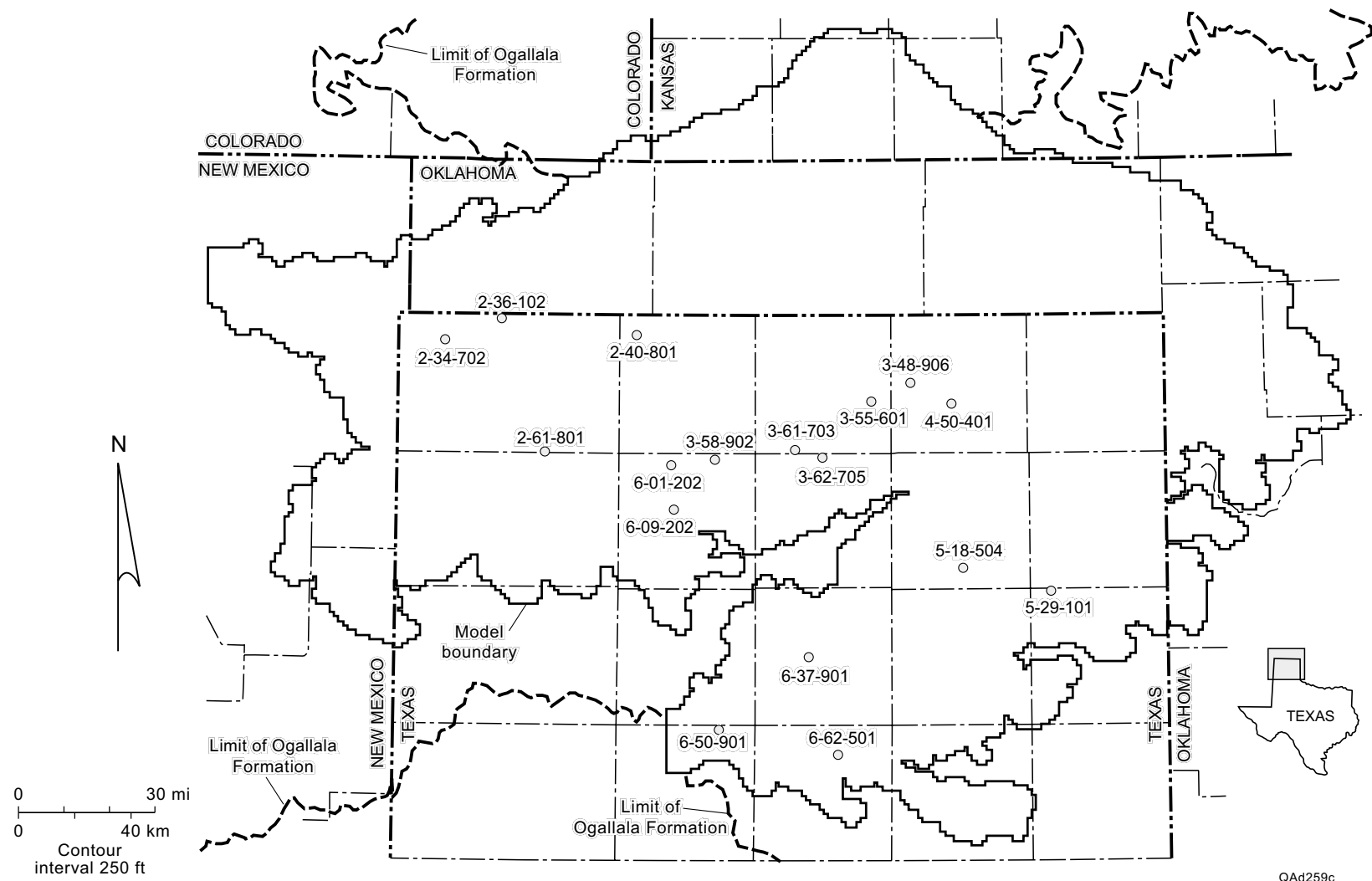


Figure 15. Map indicating location of wells with hydrographs shown in figure 11.

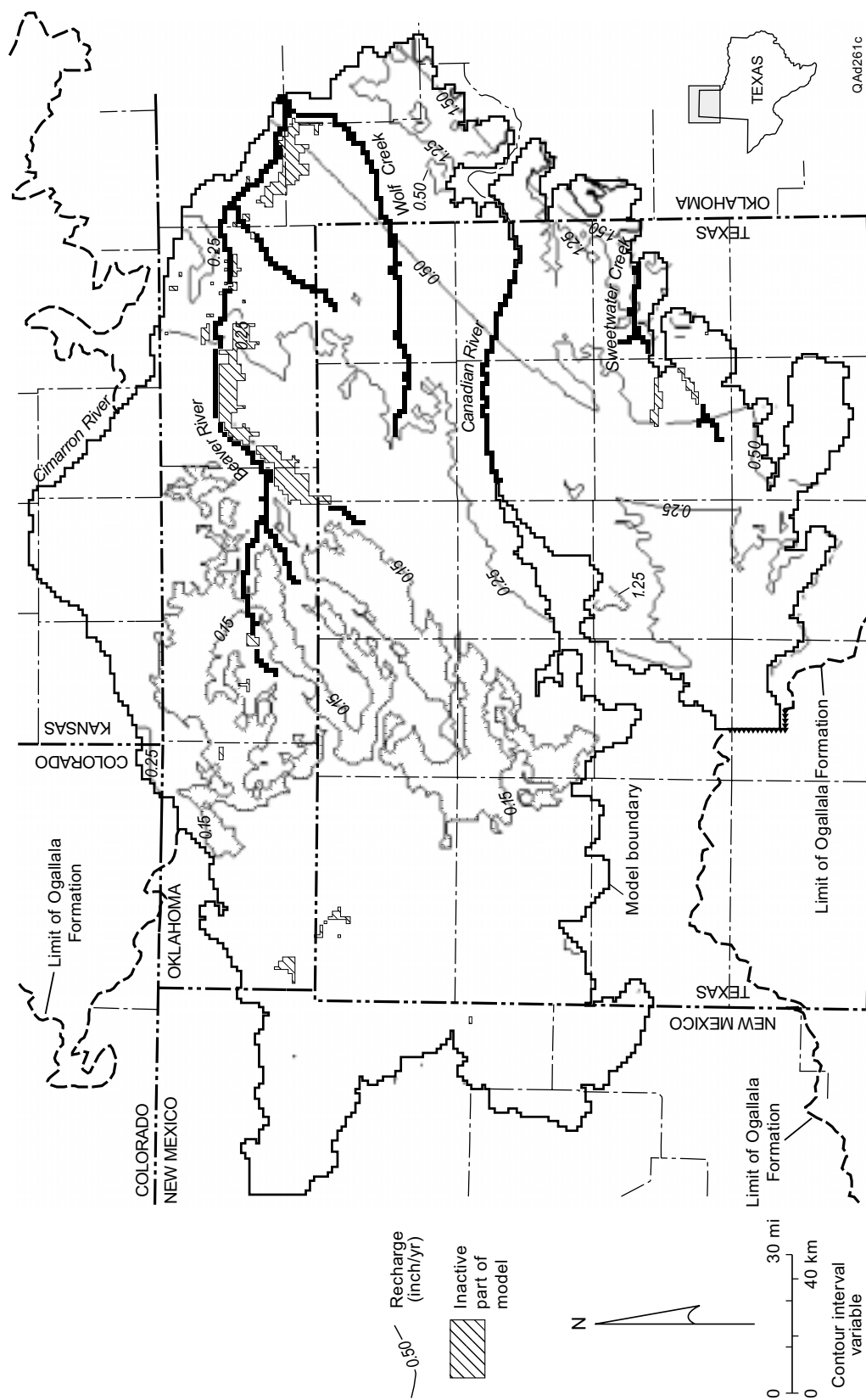


Figure 17. Recharge used in the numerical model assigned on the basis of precipitation and soil texture.

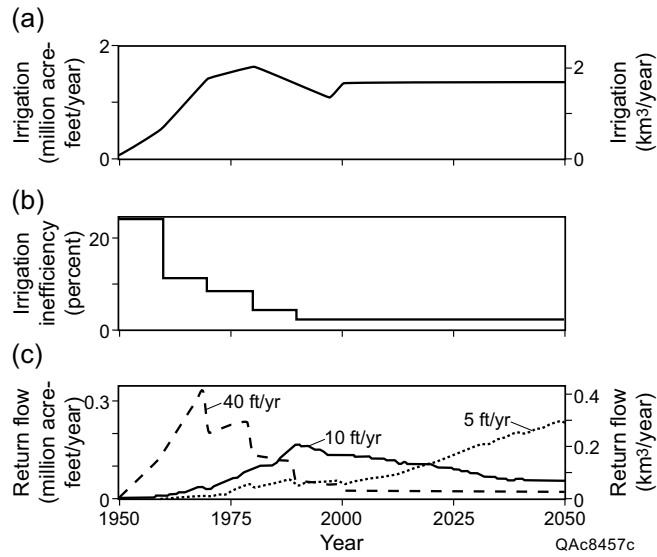


Figure 18. Estimation of return flow (c) from irrigation rates (a), inefficiency (b), and velocity at which water moves through the unsaturated zone. Inefficiency rate from Luckey and Becker (1999). Changing depth to water and soil types were also taken into account. There is no lag in return flow (c) at high velocity (e.g., 40 ft/yr [~ 12 m/yr]). At lower velocity (e.g., 5 and 10 ft/yr [1.5 and 3 m/yr]), return flow is increasingly delayed from catching the falling water table. Velocity could be less than 5 ft/yr (1.5 m/yr).

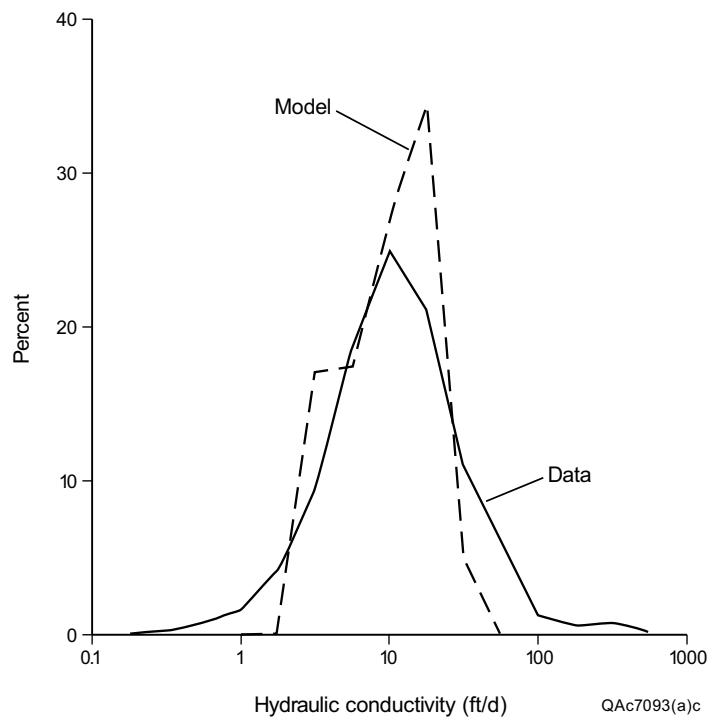


Figure 19. Comparison of measured and calibrated values of hydraulic conductivity used in the Texas part of the model.

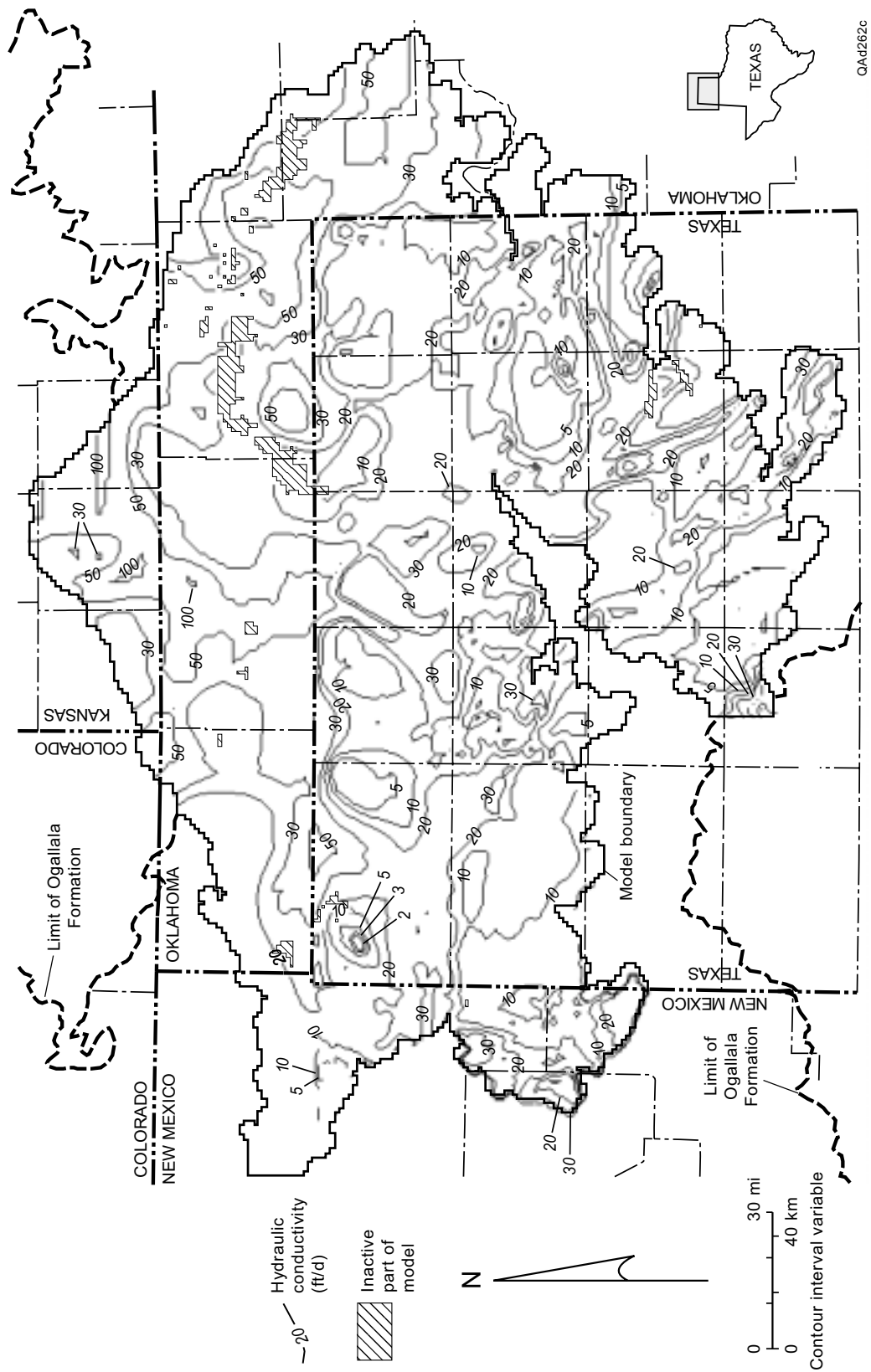


Figure 20. Hydraulic conductivity of the Ogallala aquifer used for historical and predictive simulations.